Advanced Steel Construction – Vol. 21 No. 2 (2025) 119–124
DOI:10.18057/IJASC.2025.21.2.3

PROPOSAL FOR ENHANCING THE STRUCTURAL DESIGN OF DOUBLE-SKIN TRUSS-REINFORCED COMPOSITE SHEAR WALL

Jian-Hong Han [1,*], Gan-Ping Shu [2] and Ying Qin [2]

[1] *BIM and Intelligent Construction Industry-Education Integration Research Center, School of Civil Engineering, Xinjiang Institute of Engineering, Urumqi, China*
[2] *School of Civil Engineering, Southeast University, Nanjing, China*
** (Corresponding author: E-mail: jianhong312@126.com)*

ABSTRACT

The double-skin truss-reinforced composite shear wall is a type of composite wall with steel plates connected by truss connectors. Established studies have demonstrated the improvement of compressive and shear performance of double steel plate composite shear walls by truss connectors. The structural design of truss connectors is discussed in detail in this article. The upper limit of the connector spacing-to-thickness ratio is investigated based on the elastic stability theory and the superposition principle, and a limit value of 65 k is recommended. Based on the plastic hinge theory, the existing test results and the relevant standards, the design recommendations of truss steel bar diameter and bending angle are provided. Other strengthening construction measures are also given to minimize wall damage.

ARTICLE HISTORY

Received: 5 April 2024
Revised: 26 December 2024
Accepted: 1 January 2025

KEYWORDS

Double-skin composite wall;
Truss-reinforced;
Structural design suggestion;
Spacing-to-thickness ratio;
Connectors design

1. Introduction

The double-skin composite wall is a type of composite structure composed of two steel plates, core concrete and connectors, which is first used in submarine submerged tube tunnels, nuclear containment structures, and oil or gas storage vessel structures (Wright *et al*., 1991). With its high load-bearing capacity, ease of fabrication and transportation, and the absence of the need for additional concrete forms during construction, the application of double steel plate composite walls is gradually expanding to buildings.

The strength of a double-skin composite wall depends not only on the cross-section performance of the steel plate and inner concrete, but also benefits from the combined action between the two, which is usually achieved through the bonding action between the two and the connection construction. Early axial compression test results show that for double-skin composite walls without connectors, the steel plate quickly detaches from the concrete wall at the boundary. Thus, only the compressive capacity of the concrete wall can be reflected. This results in the wall's compressive bearing capacity being significantly lower than the calculated strength of the composite members (Wright *et al*., 1995). On the contrary, the strong boundary constraint generated by the installation of the connectors allows the steel plate to work cooperatively with the concrete even after separation (Hossain *et al*., 2004). This indicates that the combined action cannot solely be achieved through bonding action but requires connectors. Consequently, double-skin composite walls with various connecters are proposed. Such as shear studs (Liang *et al*., 2004; Choi *et al*., 2014), friction welded bars (Pryer *et al*., 1998; Xie *et al*., 2007), tie bolt (Othuman *et al*., 2011; Rafiei *et al*., 2011; Zhu *et al*., 2019), enhanced C-channel connectors (Yan *et al*., 2020; Wang *et al*., 2020), J-hook connector (Liew *et al*., 2009), batten plate (Nie *et al*., 2013), L-shaped and C-shaped connectors (Chen *et al*., 2019), U-steel (Zhang *et al*., 2016), and H-steel (Guo *et al*., 2018).

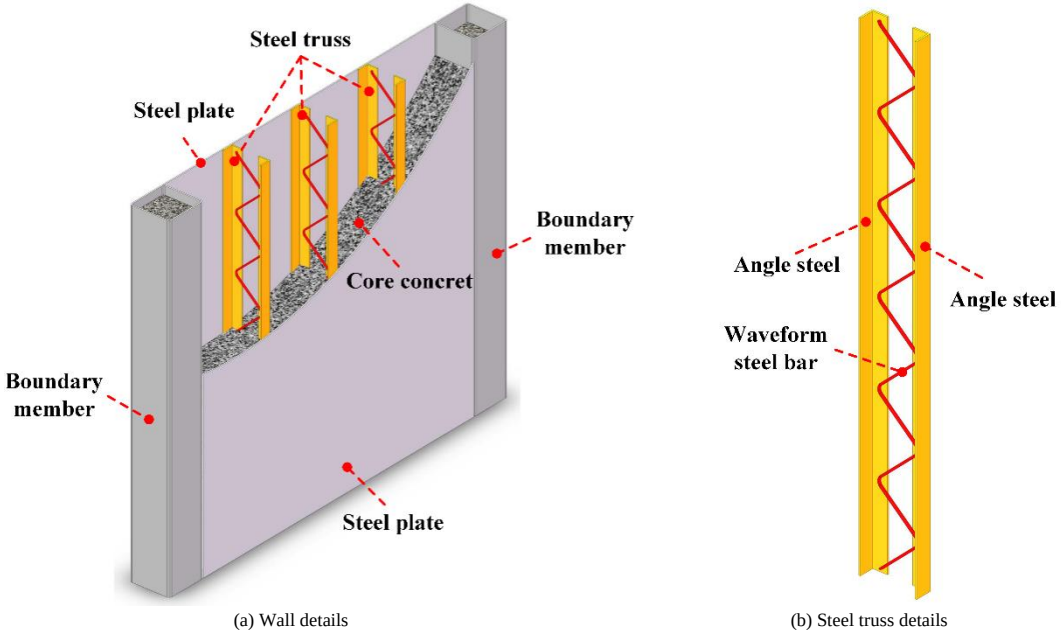

(a) Wall details (b) Steel truss details

Fig. 1 Double-skin truss-reinforced composite shear wall details

To ensure convenient construction and maintain the lateral stiffness of the wall, a double-skin composite shear wall reinforced with truss connector which is composed of angle steel and waveform steel bar was designed, as shown in Fig. 1. The truss connectors are easy to position and weld, and do not obstruct concrete flow during construction, avoiding the reduction in wall shear stiffness caused by the separation of the core concrete walls by the connectors.

Experimental research and theoretical analysis have been conducted on the compression performance (Qin *et al*., 2019; Qin *et al*., 2019; Qin *et al*., 2019) and seismic performance (Han *et al*., 2021; Han *et al*., 2021) of the double-skin truss-reinforced composite shear wall. Compared to the traditional double-skin composite wall, the truss connector also provides a strong constraint effect on both sides of the steel plate. The effects of different truss spacing on the shear bearing capacity, ductility coefficient, and buckling geometric parameters of composite walls were preliminarily studied by experiments, based on which, the design requirements for the spacing-to-thickness ratio and the truss connectors of the double-skin truss-reinforced composite shear wall were discussed in this paper.

2. Design requirements of the spacing-to-thickness ratio

As illustrated in Fig. 2, under the combined action of pressure, shear and bending moment, the buckling deformation of the strips separated by truss connectors, where a and b represent the length (or wall height H) and width (or truss connector spacing s) of the strips, respectively. At the boundaries $y = 0$ and $y = a$, the embedded effect of the core concrete wall not only restrains the relative movement of the truss connectors as steel plate stiffening ribs, but also provides them with strong torsional stiffness, and can thus be regarded as the fixed boundary of the steel plate. The boundaries $x = 0$ and $x = b$ are the loading edges for vertical pressure and horizontal shear, which can be regarded as simply supported boundaries. Therefore, the strips separated by truss connectors can be considered as narrow rectangular plates with two sides simply supported and the other two sides fixed.

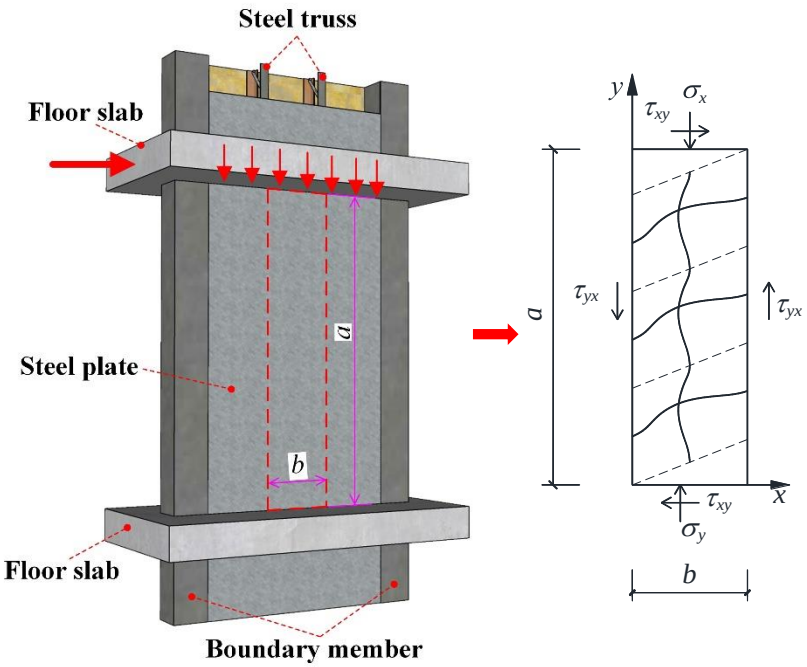

Fig. 2 Sketch of strip buckling deformation calculation

According to the energy method and superposition principle, the critical buckling normal stress σ_{cr} and shear stress τ_{cr} of a narrow rectangular plate should satisfy Eq. (1) under vertical compression and shear (Zhou, 1981):

$$\frac{\sigma_{cr}}{\sigma_{cr0}}+\left(\frac{\tau_{cr}}{\tau_{cr0}}\right)^2=1 \tag{1}$$

where, σ_{cr} and τ_{cr} are the buckling critical normal stress and shear stress under compound stress, respectively, σ_{cr0} and τ_{cr0} are the critical normal stress and shear stress of buckling under the separate action of vertical pressure and shear, which can be calculated by Eq. (2) and Eq. (3), respectively. Equation 1 shows that under the compound stress, the buckling critical normal stress and shear stress are less than the buckling critical stress under pure compression or pure shear, respectively, and the direction of the shear stress does not affect the value of the critical stress.

$$\sigma_{cr0}=k_\sigma\frac{\pi^2 D}{b^2 t_s} \tag{2}$$

$$\tau_{cr0}=k_\tau\frac{\pi^2 D}{b^2 t_s} \tag{3}$$

$$D=\frac{E_s t_s^3}{12\left(1-v^2\right)} \tag{4}$$

where, k_σ and k_τ are the buckling coefficients of vertical compression acting alone or shear acting alone, respectively; t_s are the steel plate thickness; D represents the buckling stiffness of a plate per unit width; E_s are the elastic modulus of the steel with a value of 2.06×10^5 N/mm^2; v is the Poisson's ratiowith a value of 0.3.

Introducing the critical normal stress buckling coefficients K_σ and critical shear stress buckling coefficients K_τ under composite stress, the following equations can be obtained:

$$\sigma_{cr}=K_\sigma\frac{\pi^2 D}{b^2 t_s} \tag{5}$$

$$\tau_{cr}=K_\tau\frac{\pi^2 D}{b^2 t_s} \tag{6}$$

Substituting σ_{cr}, τ_{cr}, σ_{cr0} and τ_{cr0} into Eq. (1), the relationship between buckling coefficients K_σ and K_τ can be derived as follows:

$$\frac{K_\sigma}{k_\sigma}+\left(\frac{K_\tau}{k_\tau}\right)^2=1 \tag{7}$$

Typically, the ratio of wall height to truss connector spacing, i.e. a/b, is taken to be much higher than 3.0 (this is because, for a floor height of 2700 mm, a/b less than 3.0 means that the truss connector spacing will exceed 900mm, which rarely occurs in the practical application of double-skin truss-reinforced composite shear wall). According to the values of the flexure coefficients of the two-sided simply supported two-sided fixed rectangular plate in pure compression provided in the literature (Chen, 2014) and the values of the flexure coefficients of the two-sided simply supported two-sided fixed rectangular plate in pure shear provided in the literature (Timoshenko *et al*., 1985), when a/b>3.0,

k_σ and k_τ are 6.97 and 8.99, respectively. By substituting k_σ and k_τ into Eq. 7, the relationship curve of the buckling coefficients K_σ and K_τ can be plotted as shown in Fig. 3. A portion of the buckling coefficients K_σ and K_τ are presented in Table 1.

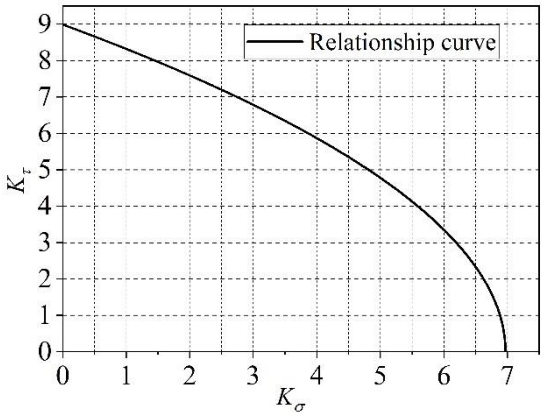

Fig. 3 Relationship curve of buckling coefficients K_σ and K_τ

Table 1
K_σ and K_τ values for the combined effect of unidirectional compression and shear

K_σ	0	1	2	3	4	5	6	6.97
K_τ	8.99	8.32	7.59	6.78	5.87	4.78	3.35	0

Limit values of b/t_s (that is, distance thickness ratio s/t_s) are discussed below. Based on the theory of shape-changing energy density, under the combined action of vertical compression and shear, the condition that the local buckling of slats does not occur before the strength yield is as follows:

$$\sqrt{\sigma_{cr}^2+3\tau_{cr}^2}\geq f_y \tag{8}$$

By Substituting σ_{cr} and τ_{cr} into Eq. (8), the following equation can be derived:

$$K_\sigma^2\left(\frac{\pi^2 D}{b^2 t_s}\right)^2+3K_\tau^2\left(\frac{\pi^2 D}{b^2 t_s}\right)^2\geq f_y^2 \tag{9}$$

According to Eq. (7),

$$K_\tau^2=k_\tau^2\left(1-\frac{K_\sigma}{k_\sigma}\right) \tag{10}$$

By Substituting K_τ^2 into Eq. (9), and defining $\beta=b/t_s$, the following equation can be derived:

$$\beta^4\leq\frac{1}{f_y^2}\left[\frac{\pi^2 E}{12\left(1-\nu^2\right)}\right]^2\left[K_\sigma^2+3k_\tau^2\left(1-\frac{K_\sigma}{k_\sigma}\right)\right] \tag{11}$$

Obviously, when the rightmost term of Eq. (11) attains its minimum value, β can obtain the minimum upper limit value. Thus, let:

$$y=K_\sigma^2+3k_\tau^2\left(1-\frac{K_\sigma}{k_\sigma}\right) \tag{12}$$

According to the extreme value theorem, y can reach a minimum value when the first-order derivative of y is equal to zero, and the second-order derivative is greater than zero, i.e.

$$\begin{cases} y'=2K_\sigma-\dfrac{3k_\tau^2}{k_\sigma}=0 \\ y''=2>0 \end{cases} \tag{13}$$

Substituting $k_\sigma=6.97$, $k_\tau=8.99$ into Eq. (13), we get $K_\sigma=17.39$. Since $K_\sigma>k_\sigma$, it indicates that under vertical pressure alone, that is, when $K_\sigma=k_\sigma$ $K_\tau=0$, β can reach the minimum limit value, thus:

$$\beta\leq\sqrt{\frac{1}{f_y}\left(\frac{\pi^2 E}{12\left(1-\nu^2\right)}\right)K_\sigma}=74.3\sqrt{\frac{235}{f_y}}=74.3\varepsilon_k \tag{14}$$

where, ε_k is the steel grade correction factor, denoted as $\sqrt{235/f_y}$.

From Eq. (14), the theoretical upper limit of spacing-to-thickness ratio (s/t_s) of truss-stiffened double steel plate combination shear wall is $74.3\varepsilon_k$. According to the test results presented in the literature (Han *et al*., 2021), specimens with a spacing-to-thickness ratio of 100 exhibit significantly lower shear bearing capacity and ductility coefficient compared to those with spacing-to-thickness ratios of 50 and 75. This indicates that the spacing-to-thickness ratio should not exceed 75, which aligns with the results from the theoretical upper limit of the spacing-to-thickness ratio calculated in Eq. (14) (where f_y=235, i.e., ε_k=1.0).

According to the "Technical Specification for Steel Plate Shear Wall" (JGJ/T 380, 2015) in China, when T-stiffeners are used for double-skin composite walls, as shown in Fig. 4, the ratio of stiffener spacing to the steel plate thickness should not exceed $60\varepsilon_k$. While for the tie bar, the ratio should not exceed $52.5\varepsilon_k$ according to the ANSI/AISC 341 (2016). It is not difficult to deduce that the truss connectors have a stronger constraint on the steel plate than the T-stiffeners or the tie bar. Therefore, the limit value for the spacing-to-thickness ratio of the double-skin truss-reinforced composite shear wall can be increased appropriately. Considering the theoretical limit and specification requirements, it is suggested that the spacing-to-thickness ratio should not exceed $65\varepsilon_k$ for double-skin truss-reinforced composite shear walls.

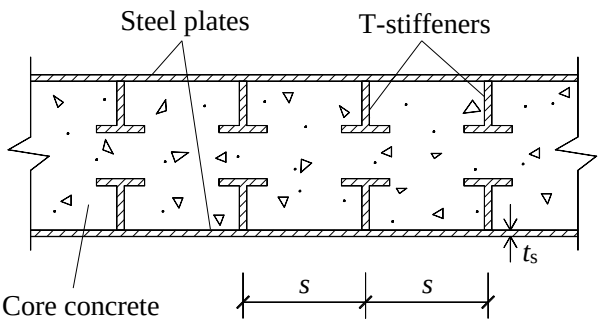

Fig. 4 Double-skin composite wall with T-stiffeners

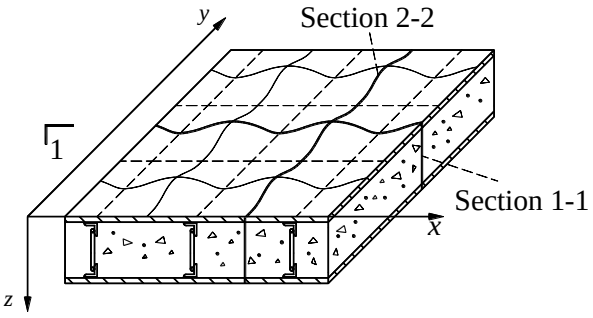

(a) Buckling deformation of steel plate-truss element

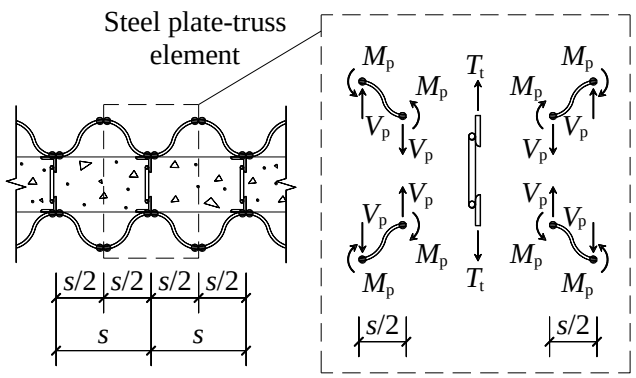

(b) Section 1-1

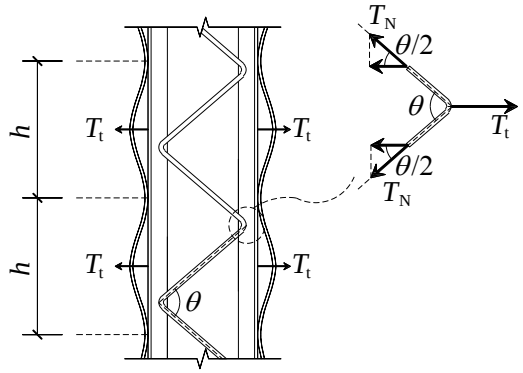

(c) Section 2-2

Fig. 5 Steel plate-truss element

3. Design requirements of the truss connector

3.1. the diameter of the waveform steel bar

Consider the steel plate-truss element shown in Fig. 5. Assume that the plastic hinge is formed at the reverse bending point when the steel plate buckles. The bending moment M_p and shear V_p at the plastic hinge section can be expressed by Eq. (15) and Eq. (16), respectively:

$$M_p = f_y \times \frac{t_s}{2} \times h \times \frac{t_s}{2} = f_y \frac{ht_s^2}{4} \tag{15}$$

$$V_p = \frac{2M_p}{(s/2)} = \frac{4M_p}{s} \tag{16}$$

Based on the force balance condition, the tension T_t of the whole truss connector can be expressed by Eq. (17):

$$T_t = 2V_p = 2f_y \frac{ht_s^2}{s} \tag{17}$$

According to the geometric relation shown in Fig. 5 (c), the tensile force T_N on the waveform steel bar can be expressed as follows:

$$T_N = \frac{T_t}{2\cos(\theta/2)} \tag{18}$$

Thus, the stress of the waveform steel bar satisfies Eq. (19) :

$$\sigma_b = \frac{T_N}{A_b} = \frac{T_t}{2\cos(\theta/2)} \times \frac{4}{\pi d_b^2} = T_t \times \frac{2}{\pi d_b^2 \cos(\theta/2)} \le f_{yb} \tag{19}$$

By Substituting Eq. (17) into Eq. (19), Eq. (20) can be derived as follows:

$$\left(2f_y \frac{ht_s^2}{s}\right) \times \frac{2}{\pi d_b^2 \cos\theta} \le f_{yb} \tag{20}$$

Therefore, the diameter d_b of the waveform steel satisfies Eq. (21).

$$d_b \ge 1.1 t_s \sqrt{\frac{h}{s} \times \frac{f_y}{f_{yb}} \times \frac{1}{\cos(\theta/2)}} \tag{21}$$

where, t_s represents the steel plate thickness, h is the height of steel plate buckling wave, s is the spacing of truss connectors, f_y represents the yield strength of steel plate, f_{yb} represents the yield strength of waveform steel bar, and θ is the bending angle of the waveform steel bar.

3.2. Buckling wave geometry characteristics

According to the literature (Han *et al*., 2021) and (Han *et al*., 2021), the statistical results of shear buckling wave geometric characteristics of each specimen are presented in Fig. 6 and Table 2. The results indicate that the ratio of buckling wave height h to the truss spacing s varies from 0.63 to 1.25, with an average value of 0.90.

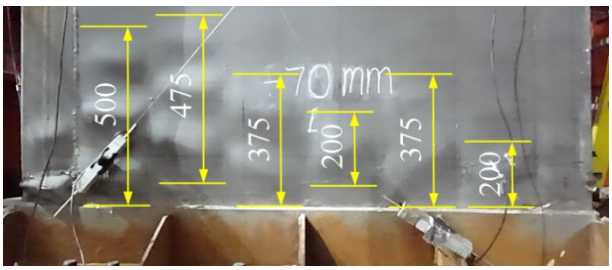

（a）SCW-1

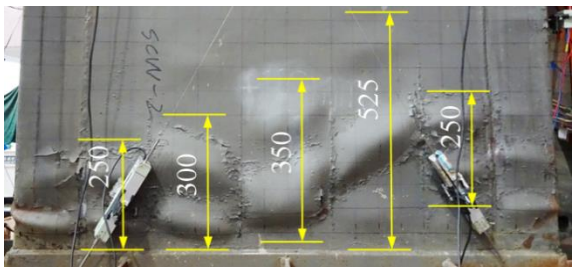

（b）SCW-2

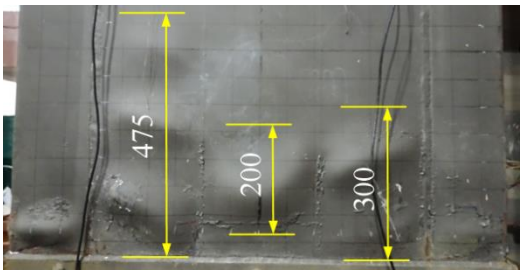

（c）SCW-3

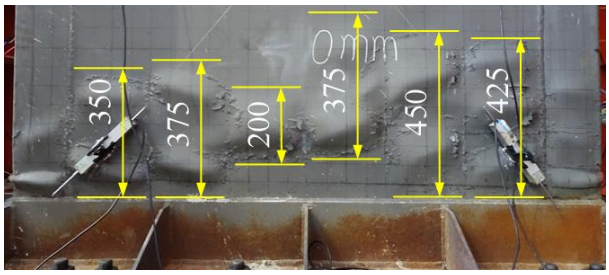

（d）SCW-4

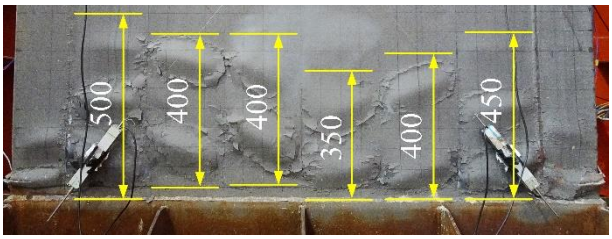

（e）SCW-5

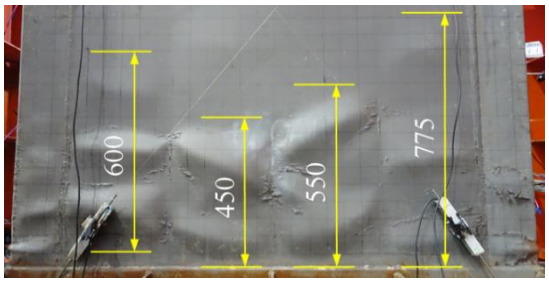

（f）SCW-6

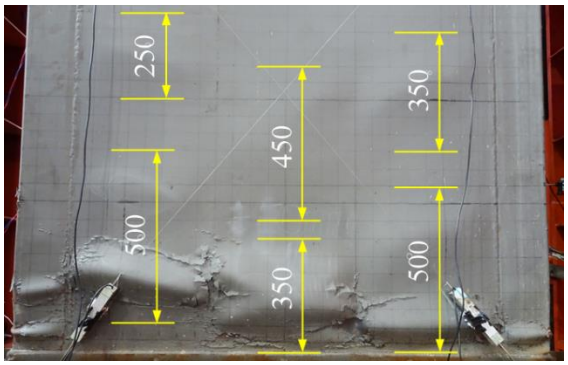

（g）SCW-7

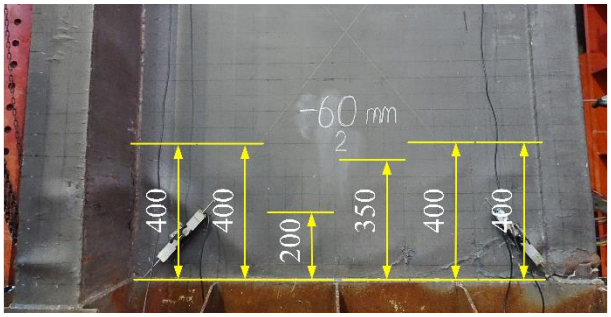

（h）SCWT-1

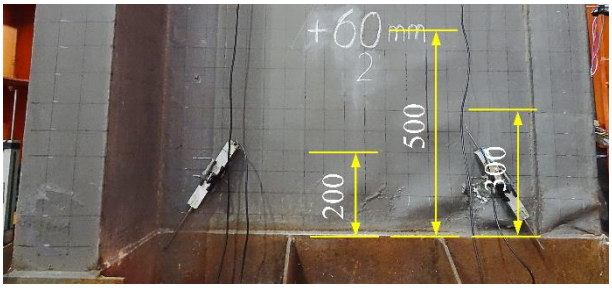

（i）SCWT-2

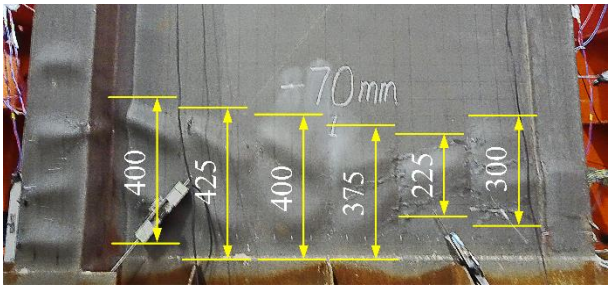

（j）SCWT-3

Fig. 6 Buckling wave height of each specimen（mm）

Table 2
Buckling wave geometry characteristics of each specimen（mm）

Specimen	Buckling wave height *h*			Spacing of truss connectors *s*	*h*/*s*		
	Maximum value	Minimum value	Average value		Maximum value	Minimum value	Average value
SCW-1	200.0	158.3	183.3	200.0	1.00	0.79	0.92
SCW-2	175.0	150.0	166.7	200.0	0.88	0.75	0.83
	125.0	125.0	125.0	150.0	0.83	0.83	0.83
SCW-3	200.0	150.0	169.4	200.0	1.00	0.75	0.85
SCW-4	225.0	141.7	186.1	200.0	1.13	0.71	0.93
SCW-5	200.0	150.0	181.9	200.0	1.00	0.88	0.91
SCW-6	275.0	200.0	239.6	300.0	0.92	0.67	0.80
SCW-7	400.0	250.0	311.1	400.0	1.00	0.63	0.78
SCWT-1	200.0	175.0	195.8	200.0	1.00	0.88	0.98
SCWT-2	250.0	166.7	205.6	200.0	1.25	0.83	1.03
	150.0	150.0	150.0	150.0	1.00	1.00	1.00
SCWT-3	225.0	150.0	195.8	200.0	1.13	0.75	0.98
Average value							0.90

3.3. Design requirements of the truss connector

To facilitate calculation, the values of parameters in Eq. (21) are specified as follows:

(1) According to the statistical results of shear buckling wave size of specimen steel plate, the average ratio of the height of buckling wave h to the spacing s of truss connectors is 0.9, i.e. h/s=0.9. Thus, Eq. (21) can be simplified to Eq. (22):

$$d_b \geq 1.0 t_s \sqrt{\frac{f_y}{f_{yb}} \times \frac{1}{\cos(\theta/2)}} \tag{22}$$

(2) According to the design specifications of steel truss size outlined in the Chinese standard "Steel-bars truss deck" (JG/T 368-2012) and "Technical specification for concrete composite slabs with lattice girders" (T/CECS 715-2020), the height of steel truss internode should be 200mm, and the width of the internode should not be less than 70mm. This requirement ensures that the bending angle of the steel bar θ does not exceed 110 degrees. In addition, to minimize steel usage, the bending angle of the waveform steel bar should be at least 90 degrees.

According to the provisions outlined above, the minimum steel bar diameter that meets the structural requirements can be calculated using Eq. (22) once the steel plate thickness, its strength grade, the waveform steel bar's strength grade, and bending angle are determined.

4. Other structural suggestions

(1) To guarantee the efficient performance of truss connectors in connecting and stabilizing the steel plate, it is recommended to use continuous fillet welds when truss connectors are connected to the steel plate.

(2) The experimental failure phenomenon demonstrates that the bottom of the boundary member, serving as the edge member in the double-skin truss-reinforced composite shear wall, is prone to buckling and tearing seriously under the influence of horizontal forces. Thus, to mitigate this issue, it is advisable to reinforce the bottom of the boundary member.

(3) In order to ensure the welding quality between steel plate and boundary member, it is suggested to appropriately increase the section width of boundary member compared to its wall thickness. The width of the rectangular steel tube should be designed to extend beyond the wall by at least 10mm on each side.

5. Conclusions

The connectors are important components that provide combined action for double steel plate combination shear walls. The truss connectors are convenient to position and weld without diminishing the shear stiffness of the wall, thereby providing adequate restraint and connection action to achieve a desirable compressive and seismic performance of the double steel plate combination shear wall. The research conducted in this paper has led to the following conclusions:

(1) Based on the theory of elastic stability and superposition principle, this study discusses the design requirements for the spacing-to-thickness ratio of double-skin truss-reinforced composite shear walls. Considering the theoretical limitations and current regulations, it is recommended that the spacing-to-thickness ratio of the double-skin truss-reinforced composite shear wall should not exceed $65\varepsilon_k$.

(2) Based on the plastic hinge theory, the diameter of the waveform steel bar in the truss connector assembly can be calculated in Eq. (21). The test results on the shear buckling wave geometric characteristics of the wall, in combination with relevant standards, have determined that a value of h/s=0.9 is taken in Eq. (21). The bending angle of waveform steel bar must have a minimum bending angle of 90 degrees.

(3) To ensure the proper connection and restraint provided by the truss connectors, continuous fillet welding should be employed between the truss connectors and the steel plates.

(4) To minimize the damage to the boundary member, it is recommended to increase the boundary member thickness or set the cladding plate to provide local reinforcement steel tube. And the boundary member should extend at least 10mm from either side of the wall.

Acknowledgments

This work is sponsored by Xinjiang Tianchi Talent Project (Grant No. 2023XGYTCYC05), the Xinjiang Uygur Autonomous Region universities basic scientific research business funds research projects (Grant No.XJEDU2022P124), and the National Natural Science Foundation of China (Grant No.52178117). The authors would like to thank the steel research group of Southeast University for their assistance with the laboratory work.

References

[1] ANSI/AISC 341-16 (2016) Specification Provisions for Structural Steel Buildings, Chicago: American Institute of Steel Construction.
[2] Chen Ji. (2014) Stability of Steel Structures Theory and Design. China Science Publishing & Media Ltd., Beijing.
[3] Chen L. H., Wang S. Y., Lou Y. (2019) Seismic behavior of double-skin composite wall with L-shaped and C-shaped connectors. *Journal of Constructional Steel Research* 160: 255-270, DOI: 10.1016/j.jcsr.2019.05.033
[4] Choi B. J., Kang C. K., Park H. Y. (2014) Strength and behavior of steel plate–concrete wall structures using ordinary and eco-oriented cement concrete under axial compression. *Thin-Walled Structures* 84: 313-324, DOI: 10.1016/j.tws.2014.07.008
[5] Guo L. H., Wang Y. H., Zhang S. (2018) Experimental study of rectangular multi-partition steel-concrete composite shear walls. *Thin-Walled Structures* 130: 577-592, DOI: 10.1016/j.tws.2018.06.011
[6] Han J. H., Shu G. P., Qin Y. (2021) Experimental seismic behavior of double skin composite wall with steel truss. *Journal of Constructional Steel Research* 180: 106569, DOI: 10.1016/j.jcsr.2021.106569
[7] Han J. H., Shu G. P., Qin Y. (2021). Experimental seismic behavior of T-shaped double skin composite wall with steel truss. *Journal of Constructional Steel Research* 184: 106776, DOI: 10.1016/j.jcsr.2021.106776
[8] Hossain K. M. A., Wright H. D. (2004) Experimental and theoretical behaviour of composite walling under in-plane shear. *Journal of Constructional Steel Research* 60(1): 59-83, DOI: 10.1016/j.jcsr.2003.08.004
[9] JGJ/T 380–2015 (2015) Technical specification for steel plate shear walls, China Architecture & building press, Beijing.
[10] JG/T 368-2012 (2012), Steel-bars truss deck, Standards Press of China, Beijing.
[11] Liang Q. Q., Uy B., Wright H. D. (2004) Local buckling of steel plates in double skin composite panels under biaxial compression and shear. *Journal of Structural Engineering* 130(3): 443-451, DOI: 10.1061/(ASCE)0733-9445(2004)130:3(443)
[12] Liew J. Y. R., Sohel K. M. A. (2009) Lightweight steel–concrete–steel sandwich system with J-hook connectors. *Engineering Structures* 31(5): 1166-1178, DOI: 10.1016/j.engstruct.2009.01.013
[13] Nie J. G., Hu H. S., Fan J. S. (2013) Experimental study on seismic behavior of high-strength concrete filled double-steel-plate composite walls. *Journal of Constructional Steel Research* 88: 206-219, DOI:10.1016/j.jcsr.2013.05.001
[14] Othuman M. M. A., Wang Y. C. (2011) Structural performance of lightweight steel-foamed concrete–steel composite walling system under compression. *Thin-Walled Structures* 49(1): 66-76, DOI: 10.1016/j.tws.2010.08.007.
[15] Pryer J. W., Bowerman H. G. (1998) The development and use of british steel Bi-steel. *Journal of Constructional Steel Research* 46(1): 173-178.
[16] Qin Y., Shu G. P., Zhou G. G. (2019) Compressive behavior of double skin composite wall with different plate thicknesses. *Journal of Constructional Steel Research* 157: 297-313, DOI: 10.1016/j.jcsr.2019.02.023
[17] Qin Y., Shu G. P., Zhou G. G. (2019) Truss spacing on innovative composite walls under compression. *Journal of Constructional Steel Research* 160: 1-15, DOI: 10.1016/j.jcsr.2019.05.027
[18] Qin Y., Shu G. P., Zhou X. L. (2019) Height-thickness ratio on axial behavior of composite wall with truss connector. *Steel and Composite Structures* Feb 25;30(4):315–325, DOI: 10.12989/scs.2019.30.4.315
[19] Rafiei S. (2011) Behaviour of double skin profiled composite shear wall system under in-plane monotonic, cyclic and impact loadings. Ph. D. thesis, Ryerson University, Toronto, Canada.
[20] Stephen P. Timoshenko, James M. Gere. (1985) Theory of Elastic Stability. Koon Wan Printing Pte. Ltd.
[21] T/CECS 715-2020 (2020), Technical specification for concrete composite slabs with lattice girders, China Architecture & building press, Beijing.
[22] Wright H. D., Gallocher S. C. (1995) The behaviour of composite walling under construction and service loading. *Journal of Constructional Steel Research* 35(3): 257-273.
[23] Wright H. D., Oduyemi T. O. S., Evans H. R. (1991) The design of double skin composite elements. *Journal of Constructional Steel Research* 19(2): 111-132.
[24] Wang T., Yan J. B. (2020) Developments of steel-concrete-steel sandwich composite structures with novel EC connectors: Members. *Journal of Constructional Steel Research* 175: 106335, DOI: 10.1016/j.jcsr.2020.106335
[25] Xie M., Foundoukos N., Chapman J. C. (2007) Static tests on steel–concrete–steel sandwich beams. *Journal of Constructional Steel Research* 63(6): 735-750, DOI: 10.1016/j.jcsr.2006.08.001
[26] Yan J. B., Chen., Wang T. (2020) Compressive behaviours of steel-UHPC-steel sandwich composite walls using novel EC connectors. *Journal of Constructional Steel Research* 173: 106244. DOI: 10.1016/j.jcsr.2020.106244
[27] Zhang X. M., Qin Y., Chen Z. H. (2016) Experimental seismic behavior of innovative composite shear walls. *Journal of Constructional Steel Research* 116: 218-232, DOI: 10.1016/j.jcsr.2015.09.015
[28] Zhou Ch. T. (1981) Elastic stability theory. Sichuan People's Publishing House, Sichuan.
[29] Zhu J. S., Guo Y. L., Wang M. Z. (2019) Strength design of concrete-infilled double steel corrugated-plate walls under uniform compressions. *Thin-Walled Structures* 141: 153-174, DOI: 10.1016/j.tws.2019.02.021